# Tensor Renormalization Group Study of the General Spin-S Blume–Capel Model

Li-Ping Yang[1,2*] and Zhi-Yuan Xie[3,4]

[1]*Department of Physics, Chongqing University, Chongqing 401331, China*
[2]*Beijing Computational Science Research Center, Beijing 100193, China*
[3]*Department of Physics, Renmin University of China, Beijing 100872, China*
[4]*Institute of Physics, Chinese Academy of Sciences, Beijing 100190, China*

We focus on the special situation of $D = 2J$ in the general spin-S Blume–Capel model on a square lattice. Under an infinitesimal external magnetic field, the phase transition behaviors due to the thermal fluctuations are investigated by the newly developed tensor renormalization group method. We clearly demonstrate the phase transition process: in the case of an integer spin-S, there are $S$ first-order phase transitions with the stepwise magnetizations $M = S, S - 1, \ldots, 0$; in the case of a half-odd integer spin-S, there are $S - 1/2$ first-order phase transitions with corresponding $M = S, S - 1, \ldots, 1/2$ in addition to one continuous phase transition due to spin-flip $Z_2$ symmetry breaking. At low temperatures, all first-order phase transitions are accompanied by the successive disappearance of the spin-component pairs ($\pm s$); furthermore, the transition temperature for the nth first-order phase transition is the same, independent of the value of the spin-S. In the absence of a magnetic field, a visualization parameter characterizing the intrinsic degeneracy of the different phases provides a different reference for the phase transition process.

## 1. Introduction

The Blume–Capel model[1] and the extended Blume–Emery–Griffiths model[2] have attracted general interest over several decades. The Monte Carlo algorithm,[3–5] conformal invariance,[4] finite-size scaling[6] and mean-field approximation[7,8] demonstrate the rich phase diagrams based on this model. The richness originates not only from spin-flip $Z_2$ symmetry breaking, but also from density fluctuations with $S + 1$ (for integer $S$) or $S + 1/2$ (for half-odd integer $S$) possible values[7] for $S_i^2$. Furthermore, these models give a characterization for experimental 3He–4He mixtures[9,10] and metamagnets,[11] which inspired the vector version[12,13] of these models. The introduction of bond randomness[14,15] further enriches the phase transition discussion.

The Hamiltonian of the Blume–Capel model[1] with a general spin-S is

$$H = -J \sum_{\langle i,j \rangle} S_i S_j + D \sum_i S_i^2 - h \sum_i S_i^z, \qquad (1)$$

where the spin variable $S$ takes $2S + 1$ values ($-S$, $-S + 1, \ldots, S - 1, S$). $J$ is the coupling constant, $D$ is the strength of the single-ion anisotropy, and $h$ is the magnetic field. The sum of the first term runs over all the nearest neighbors.

Firstly, we consider the case of $h = 0$. When $D = 0$, this model is reduced to the classical Ising model. When $D$ approaches positive infinity, the energy-favorable state is the one with the full occupation of the smallest spin component. For the integer spin cases, the component is $S = 0$. For the half-odd integer cases, the component is $S = \pm 1/2$.

If we look at the Hamiltonian of any bond linking two sites $i, j$, then we have

$$H_{ij} = -J S_i S_j + D(S_i^2 + S_j^2)/q. \qquad (2)$$

Here, $q$ is the coordination number, which depends on the lattice structure. This formula can be rewritten as

$$H_{ij} = J(S_i - S_j)^2/2 + (D/q - J/2)(S_i^2 + S_j^2), \qquad (3)$$

which leads to the following conclusions for the ferromagnetic coupling ($J > 0$): when $D > qJ/2$, the configuration of the ground state is $S_i = S_j = 0$ (integer spin) and $S_i = S_j = \pm 1/2$ (depending on the spontaneous breaking of the half-odd integer spin), respectively, for the integer and half-odd spin-S cases; when $D < qJ/2$, the configuration of the ground state is $S_i = S_j = \max(S)$ for any spin-S case.

As a result, we have a special situation, i.e., $D = qJ/2$, where the ground state is $S_i = S_j$ with $(2S + 1)$-fold degeneracy. If An infinitesimal field $h$ is applied, then the ground-state degeneracy will be lifted. The positive infinitesimal $h$ makes the system enter the ground state with $S_i = S_j = \max(S)$ as in the case of $D < qJ/2$, $h = 0$.

Without loss of generality, we focus on a square lattice hereafter. Then, $q = 4$ and $D = 2J$ are the special parameters. The phase boundary of the square lattice[3,4,6,8] ends at $(T/J, D/J) = (0, 2)$, i.e., the transition temperature is $T_t = 0$ for the general spin cases when $h = 0$, $D = 2J$.

Motivated by the special parameter point and curiosity about how the phase boundary approaches the end point, we calculate the thermodynamic behaviors of the model described by Eq. (1). Using the recently developed tensor renormalization group algorithm,[16] this work demonstrates and visualizes the phase transition process in terms of the common and special physical quantities.

For a classical lattice model with local interactions, the partition function can be represented as a fourth-order tensor product,[17]

$$Z = \text{Tr} \prod_i T_{l_i r_i u_i d_i}, \qquad (4)$$

where $i$ runs over all the lattice sites and Tr denotes the summation over all bond indices. The local tensor $T$ is defined at each lattice site as shown in Fig. 1, and the indices $l$, $r$, $u$, $d$ mean the left, right, up, and down directions, respectively. Here, the initial tensor $T$ is an order-4 tensor due to the four indices. The initial dimension $d_0 = (2S + 1)$ of each order is the degree of freedom for the spin. Detailed information about the construction of the tensor can be found in Refs. 17 and 18.
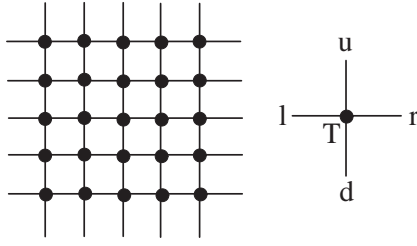
**Fig. 1.** Graphical representation of the tensor network (left) and the fourth-order tensor defined at each site (right).

$$T_{l_i r_i u_i d_i} = \sum_\alpha W_{\alpha l_i} W_{\alpha r_i} W_{\alpha u_i} W_{\alpha d_i}. \tag{5}$$

$W$ originates from the decomposition of the bond matrix $A_{S_i S_j} = e^{-\beta H_{S_i S_j}}$, i.e., $A = WW^\dagger$. Here,

$$H_{S_i S_j} = -J S_i S_j + D(S_i^2 + S_j^2)/q - h(S_i + S_j)/q. \tag{6}$$

To contract the tensor network, i.e., trace over all sites, we face the problem of the exponentially increasing dimension of each order of the tensor. The bond dimensions of the $n$th and $(n-1)$th contractions satisfy $d_n = d_{n-1}^2$. The contraction process rapidly makes the dimension inaccessible. In 2007, Levin and Nave proposed a cutoff scheme[19] based on singular value decomposition (SVD) that uses an affordable cutoff dimension $d$ to obtain a good approximation for the partition function, by which the thermodynamic properties of the system can consequently be obtained.

Recently, we proposed a novel coarse-graining tensor renormalization group (TRG) algorithm based on high-order singular value decomposition (HOSVD),[20,21] abbreviated to HOTRG, which provides an accurate but low-computational-cost technique for studying two- or three-dimensional (3D) lattice models. The coarse-graining procedure consists of iteratively replacing blocks of size two by a single site by using HOSVD along the horizontal ($x$-axis) and vertical ($y$-axis) directions alternately.

The following results are all from the newly developed HOTRG scheme. Hereafter, the coupling constant $J$ is used as the energy unit and $k_B$ is set as 1. In the calculation of the magnetization and the occupation number, $h$ is taken as $10^{-10}$ in Eq. (1) for the preferential symmetry breaking of the spin pairs ($\pm s$) and computational stability. The infinitesimal $h$ ensures the correspondence with the case of $h = 0$, $D = 2J - \epsilon$. Here, $\epsilon$ is a positive infinitesimal number.

The system size is $2^{N_s}$ and we fix $N_s = 40$ for the calculation of the thermodynamic physical quantities. However, $h$ is fixed at 0 and $N_s$ takes different values for the calculation of the visualization parameter[22] depending on the state degeneracy, which will be addressed in Sect. 4. The periodic boundary condition is adopted in the entire numerical calculation.

In the following, we will discuss the results for the typical integer cases of $S = 1, 2$ in Sect. 2 and the half-odd integer cases of $S = 3/2, 5/2$ in Sect. 3. Then we analyze the visualization parameter of the phase transition in Sect. 4. Finally, we give a conclusion.

## 2. Integer Cases: $S = 1, 2$

In the case of $S = 1$, there are three possible spin values,
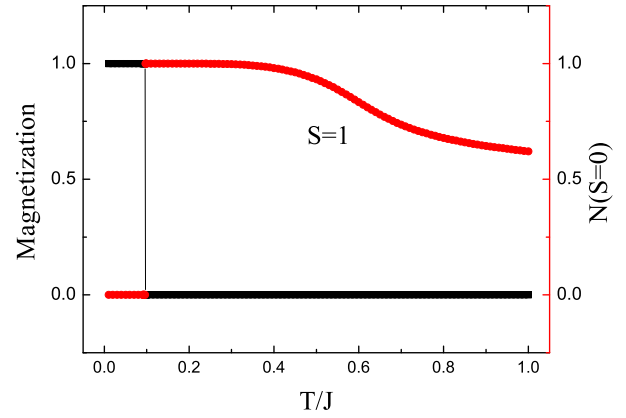


**Fig. 2.** (Color online) Temperature dependences of the magnetization (black lines) and occupation number $N(S = 0)$ (red lines, light gray line). Here, $S = 1$, $D = 2J$, $N_s = 40$, $d = 30$, $h = 10^{-10}$.

$\pm 1, 0$, for each spin variable. A tricritical point exists, enriching the phase diagram.

In the limit of infinite $D$, the energy-favorable state is the full occupation of $S = 0$, denoted as $N(S = 0) = 1$ per site. We can name $S = 0$ as the vacancy or hole, and the state full of holes is simply the hole condensed phase, whose quantum correspondence is the one-dimensional $S = 1$ quantum model with single-ion anisotropy in our previous papers.[23,24] The hole condensed states also emerge in the other general integer spin-S cases.

As shown in Fig. 2, the system undergoes first-order phase transitions accompanying the emergence of the hole condensed phase as the temperature varies. The magnetization jumps from 1 to 0 at a location consistent with the kink of the occupation number of the pair $N(S = \pm1)$. The transition point is $T_t = 0.096$. For the plateau of the magnetization $M = 0$, the starting point corresponds to the condensation of the holes with the disappearance of the pair $S = \pm1$. With further increasing temperature, the components $S = \pm1$ return to the system with equal-weight occupation, and the system enters the paramagnetic state with magnetization $M = 0$. In the limit of the high temperature, the occupation numbers of the three different components $S = 1, 0, -1$ all become $1/3$.

For the case of $S = 2$, there are five possible spin values, $0, \pm1, \pm2$, for the spin variable. Compared with the case of $S = 1$, there is one more possible pair, $S = \pm2$, which induces one more jump of the magnetization from $M = 2$ to 1. The system undergoes two first-order phase transitions with increasing temperature.

The first plateau $M = 2$ corresponds to the full occupation of $S = 2$ from the breaking of the pair $S = \pm2$ due to the infinitesimal magnetic field $h$. As shown in Fig. 3, the second plateau $M = 1$ emerges with the disappearance of $S = \pm2$ and the full occupation of $S = 1$ from the breaking of the pair $S = \pm1$. The second jump of the magnetization occurs with the hole condensed phase $N(S = 0) = 0$. With further increasing temperature, the occupation of the hole decreases continuously. The degrees of freedom $S = \pm1$ and $\pm2$ gradually return to the system. $N(S = 0) + N(S = \pm1) \simeq 1$ holds up to a high temperature. Accompanying the successive disappearances of $S = \pm2$ and $\pm1$, the two transition points are located at $T_{t_1} = 0.096$ and $T_{t_2} = 0.305$, respectively.
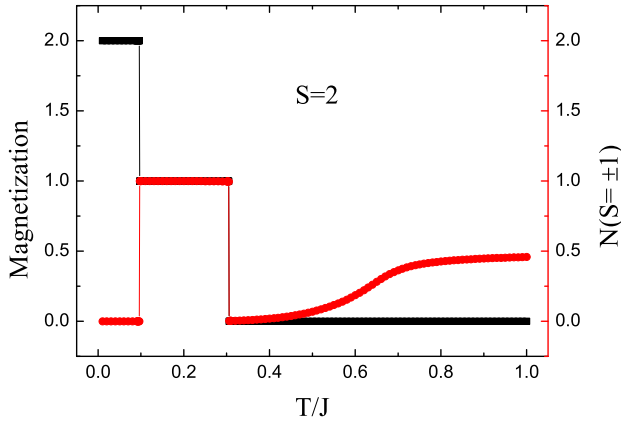
**Fig. 3.** (Color online) Magnetization (black lines) and occupation number $N(S = \pm 1)$ (red lines, light gray line) as a function of the reduced temperature $T/J$. Here, $S = 2$, $D = 2J$, $N_s = 40$, $d = 30$, $h = 10^{-10}$.
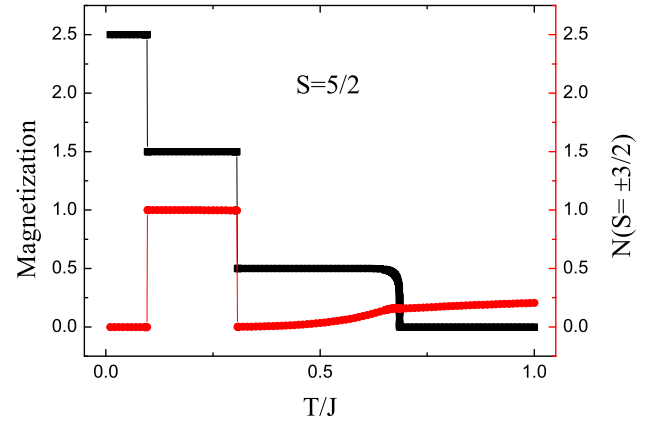


**Fig. 5.** (Color online) Temperature dependence of the magnetization (black lines) and occupation number $N(S = \pm 3/2)$ (red lines, light gray line). Here, $S = 5/2$, $D = 2J$, $N_s = 40$, $d = 40$, $h = 10^{-10}$.



**Fig. 4.** (Color online) Temperature dependence of the magnetization (black lines) and occupation number $N(S = \pm 1/2)$ (red lines, light gray line). Here, $S = 3/2$, $D = 2J$, $N_s = 40$, $d = 40$, $h = 10^{-10}$.
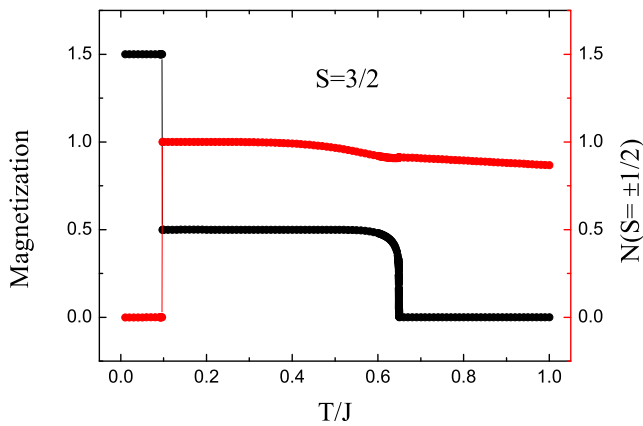
## 3. Half-Odd Cases: $S = 3/2, 5/2$

For $S = 3/2$, there are four possible spin values, $\pm 3/2$, $\pm 1/2$, for each spin variable.

Similar to the case of $S = 1$, the system breaks into the state with $M = 3/2$ due to the infinitesimal $h$. The first jump from $M = 3/2$ to $1/2$ exhibits competition of the occupation of two pairs between $S = \pm 3/2$ and $\pm 1/2$. The first-order phase transition changes the full occupation from $S = 3/2$ to $1/2$.

When the temperature increases further, an Ising-like continuous phase transition due to spin-flip $Z_2$ symmetry breaking occurs. From the behaviors of the magnetization shown in Fig. 4, the two transition points are located at $T_{t_1} = 0.096$ and $T_{t_2} = 0.649$. The location of $T_{t_2}$ is close to the data shown in Fig. 2 in Ref. 4.

A similar discussion is applied to the case of $S = 5/2$, where there are six possible spin values, $\pm 1/2, \pm 3/2, \pm 5/2$, for each spin variable.

The first two jumps in the magnetization correspond to first-order phase transitions. The successive symmetry breaking of the pairs $(\pm s)$ is clearly shown in the profile of the occupation number $N(S = \pm 3/2)$. At the first plateau $M = 5/2$, the degrees of freedom $S = (\pm 3/2, \pm 1/2)$ disappear.

With increasing temperature, the first jump of $M$ and $N$ indicates the disappearance of $S = \pm 5/2$ and the full occupation of $S = \pm 3/2$. Then the second jump of $M$ and $N$ represents the ensuing replacement of $S = \pm 3/2$ by $S = \pm 1/2$ as shown in Fig. 5. The symmetry breaking of the spin pair $S = \pm 1/2$ due to magnetic field $h$ results in $N(S = 1/2) = 1$.

However, with further increasing temperature, $M$ decreases to 0 continuously, and the system enters the paramagnetic phase. Here, the occupation number $N(S = \pm 3/2)$ increases continuously from 0. The extra calculation shows that $N(S = 1/2) = N(S = -1/2)$ and $N(S = 3/2) = N(S = -3/2)$ in the paramagnetic phase, where $N(S = \pm 1/2) + N(S = \pm 3/2) \simeq 1$ holds up to a high temperature until the equal weight distribution of all the degrees of freedom in the high-temperature limit. The three transition points are $T_{t_1} = 0.096$, $T_{t_2} = 0.306$, and $T_{t_3} = 0.685$.

Reviewing the data for the transition points, we find that the transition temperature for the 1st first-order phase transition is fixed at $T_{t_1} = 0.096$ for the above four cases of $S = 1, 3/2, 2, 5/2$ and the 2nd first-order phase transition is located at $T_{t_2} = 0.305$ (0.306) for $S = 2$ (5/2).

Let us turn to the principle of the minimal free energy, $F = U - TS$. The phase transition occurs during the competition between the internal energy and the entropy. Assuming that there are two clusters separately filled with single spin components $s, s - 1$, the existence of an interface connecting the two clusters will raise the internal energy. Simultaneously the entropy is increased as a result of the larger number of possible configurations. The 1st first-order phase transition occurs with the global spin-component replacement of $S$ by $S - 1$ in each site, and the transition point is irrelevant of the value of spin-$S$. A similar discussion applies to nth first-order phase transition in the low-temperature situation. The same interval between spin components results in the same internal energy difference. For low temperatures, the relative Boltzmann weight $e^{-\beta \Delta E}$ due to the variation of the spin components is negligible. As a consequence, we cannot see appreciable thermal fluctuations, then a magnetization plateau emerges.

An additional check shows that the position of the 1st first-order phase transition moves closer to zero temperature with smaller $h$. However, the continuous phase transition points

are insensitive to the magnitude of the infinitesimal $h$. At relatively high temperatures, the effect from the infinitesimal $h$ is negligible. Our results for the continuous phase transition points, $T_t = 0.649, 0.685$ for $S = 3/2, 5/2$, respectively, can be used as reference data. All 1st first-order phase transitions will occur at zero temperature for the exact $D = 2J$, $h = 0$ situation, which is a spontaneous symmetry-breaking picture in the thermodynamic limit and exactly demonstrated in Ref. 8.

Nevertheless, the strength of $h$ does not change the fact that the corresponding location of the nth first-order phase transition remains the same, independent of the spin values at low temperatures although the infinitesimal $h$ shifts the transition point along the temperature axis. Furthermore, the novel perspective obtained from the visualization parameter[22] also provides qualitative consistency.

## 4. Visualization Parameter

As was pointed out in Ref. 22, a symmetry-breaking phase with $n$ degenerate states is represented by a fixed-point tensor, which is a direct sum of $n$ one-dimensional trivial tensors. $X_1$ is here introduced to visualize the structure of fixed-point tensor with the following definition:

$$X_1 = \frac{\left( \sum_{ru} T_{ruru} \right)^2}{\sum_{ruld} T_{rulu} T_{ldrd}}. \tag{7}$$

$X_1$ is independent of the scale of the tensor, and a graphical representation is given in Fig. 13 of Ref. 22. $X_1$ directly represents the information of the degeneracy associated with the symmetry underlying the Hamiltonian.

For the integer case of $S = 2$, the visualization $X_1$ bears the stepwise structure $5, 3, 1$ as shown in Fig. 6. The five-fold degeneracy associated with $T^{Z_2} \bigoplus T^{Z_2} \bigoplus T^{TRI}$ is represented by the first plateau with a value of 5. $T^{Z_2}$ corresponds to the spin flip of the pair $(\pm s)$ and $T^{TRI}$ originates from the degree of freedom $S = 0$. With increasing temperature, the system undergoes two phase transitions. The first jump of $X_1$ from 5 to 3 indicates the disappearance of $T^{Z_2}$ from $S = \pm 2$, where $N(S = 1)$ exhibits the step change from 0 to 1. The plateau of $X_1 = 3$ corresponds to $T^{Z_2} \bigoplus T^{TRI}$ referring to $S = 0, 1, -1$. With the consequent disappearance of $T^{Z_2}$ from $S = \pm 1$, the plateau of $X_1 = 1$ with $N(S = 0) = 1$ occurs.

$X_1$ is used to characterize the degeneracy, which is the reason why $h$ is fixed at 0 here. The introduction of $h$ lifts the degeneracy. Even a tiny numerical calculation error will affect the numerical results for the intrinsic degeneracy. We choose different system sizes of $2^{N_s}$ ($N_s = 20, 30, 40$) for comparison. With increasing $N_s$, the transition points move to the left, corresponding to a lower transition temperature. The first transition point should be $T_t = 0$ when $D = 2J$, $h = 0$. On the other hand, a large system size will result in numerical instability for $X_1$ with more coarse-graining steps, as shown in Fig. 7. When the symmetry describing the state degeneracy is not implemented in the construction of the original tensor, we will face the problem of numerical instability. By implementing U(1) symmetry in the initial tensor construction of O(2) model,[25] the numerical results with high precision are obtained. Research on the fixed-point tensor is still under way.
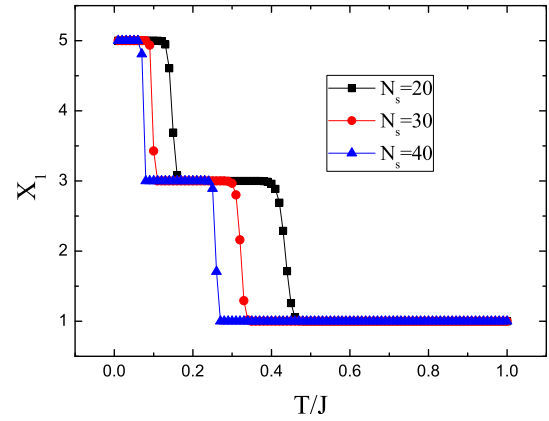


**Fig. 6.** (Color online) Stepwise structure of the visualization $X_1$ with three plateaus $(5, 3, 1)$ as a function of the reduced temperature $T/J$. Three different lattice sizes, $N_s = 20, 30, 40$, are compared. Here, $S = 2$, $D = 2J$, $d = 40$, $h = 0$.
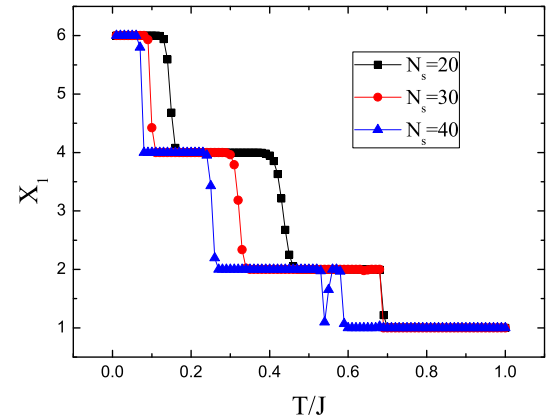


**Fig. 7.** (Color online) Stepwise structure of the visualization $X_1$ with four plateaus $(6, 4, 2, 1)$ as a function of the reduced temperature $T/J$. Three different lattice sizes, $N_s = 20, 30, 40$, are compared. Here, $S = 5/2$, $D = 2J$, $d = 40$, $h = 0$.

For the half-odd case of $S = 5/2$, the visualization $X_1$ bears the stepwise structure $6, 4, 2, 1$, as shown in Fig. 7. The six-fold degeneracy originates from three pairs $\pm 5/2$, $\pm 3/2, \pm 1/2$, corresponding to $T^{Z_2} \bigoplus T^{Z_2} \bigoplus T^{Z_2}$. The first two jumps of $X_1$ represent the two first-order phase transitions, which are similar to those in the case of $S = 2$ accompanying the successive disappearance of the two pairs. The difference lies in the last jump of $X_1$ from 2 to 1, which is a continuous phase transition with $Z_2$ spin-flip symmetry breaking. The gap of $X_1$ is 2 for all the first-order phase transitions and 1 for the last continuous Ising-like phase transition.

The above discussion leads to the general conclusion that the visualization parameter $X_1$ bears the stepwise structure $(2S + 1, 2S - 1, \ldots, 3, 1)$ for the integer spin $S$ and $(2S + 1, 2S - 1, \ldots, 2, 1)$ for the half-odd spin $S$. It is tricky to locate the transition point from the jump of $X_1$ due to the truncation in the coarse-graining process. However, the point that the integer plateaus of $X_1$ associated with the degeneracy of the system is intrinsic, which originates from the deep insight that the fixed-point of the tensor representation corresponds to the fixed point of the RG flow. This provides reference to observe the phase transition. By implementing

the symmetry in the initial tensor construction, the phase transition point of ferromagnetic potts models on a simple cubic lattice identified by $X_1$ can outperform the most recent Monte Carlo result.[26]

## 5. Conclusion

In summary, we discussed the phase transitions of the Blume–Capel model on a square lattice using the recently developed HOTRG. The case of $h = 0$, $D = 2J$ is a special situation with high energy degeneracy, where the bond Hamiltonian has the form of the square sum. When an infinitesimal $h$ with the same magnitude is applied, at low temperatures the location of the nth first-order phase transition is the same, independent of the spin-S. The positions of the successive phase transitions can be identified more exactly by increasing the cutoff dimension $d$. Through the magnetization and the occupation number of different spin values, the phase transition behaviors are clearly demonstrated, and are consistent with the mean-field solution.[8] The visualization parameter $X_1$ associated with the degeneracy illustrates the successive phase transitions. Compared with the integer spin-S cases, there is one more Ising-like continuous phase transition with spin-flip $Z_2$ symmetry breaking for half-odd spin-S cases.

### Acknowledgments

*liping2012@cqu.edu.cn
1) M. Blume, Phys. Rev. **141**, 517 (1966); H. W. Capel, Physica **32**, 966 (1966).
2) M. Blume, V. J. Emery, and R. B. Griffiths, Phys. Rev. A **4**, 1071 (1971).
3) C. J. Silva, A. A. Caparica, and J. A. Plascak, Phys. Rev. E **73**, 036702 (2006).
4) J. C. Xavier, F. C. Alcaraz, D. Penã Lara, and J. A. Plascak, Phys. Rev. B **57**, 11575 (1998).
5) W. Kwak, J. Jeong, J. Lee, and D.-H. Kim, Phys. Rev. E **92**, 022134 (2015).
6) P. D. Beale, Phys. Rev. B **33**, 1717 (1986).
7) W. Hoston and A. N. Berker, Phys. Rev. Lett. **67**, 1027 (1991).
8) J. A. Plascak, J. G. Moreira, and F. C. Sá Barreto, Phys. Lett. A **173**, 360 (1993).
9) E. H. Graf, D. M. Lee, and J. D. Reppy, Phys. Rev. Lett. **19**, 417 (1967).
10) G. Goellner and H. Meyer, Phys. Rev. Lett. **26**, 1534 (1971).
11) V. A. Schmidt and S. A. Friedberg, Phys. Rev. B **1**, 2250 (1970).
12) J. L. Cardy and D. J. Scalapino, Phys. Rev. B **19**, 1428 (1979).
13) A. N. Berker and D. R. Nelson, Phys. Rev. B **19**, 2488 (1979).
14) A. Malakis, A. N. Berker, I. A. Hadjiagapiou, and N. G. Fytas, Phys. Rev. E **79**, 011125 (2009).
15) A. Malakis, A. N. Berker, I. A. Hadjiagapiou, N. G. Fytas, and T. Papakonstantinou, Phys. Rev. E **81**, 041105 (2010).
16) Z. Y. Xie, J. Chen, M. P. Qin, J. W. Zhu, L. P. Yang, and T. Xiang, Phys. Rev. B **86**, 045139 (2012).
17) H. H. Zhao, Z. Y. Xie, Q. N. Chen, Z. C. Wei, J. W. Cai, and T. Xiang, Phys. Rev. B **81**, 174411 (2010).
18) Z. Y. Xie, H. C. Jiang, Q. N. Chen, Z. Y. Weng, and T. Xiang, Phys. Rev. Lett. **103**, 160601 (2009).
19) M. Levin and C. P. Nave, Phys. Rev. Lett. **99**, 120601 (2007).
20) L. De Lathauwer, B. De Moor, and J. Vandewalle, SIAM J. Matrix Anal. Appl. **21**, 1253 (2000).
21) D. Luo, C. Ding, and H. Huang, in *Advances in Knowledge Discovery and Data Mining*, ed. J. Z. Huang, L. Cao, and J. Srivastava (Springer, Berlin, 2011) Part I, p. 148; G. Bergqvist and E. G. Larsson, IEEE Signal Process. Mag. **27**, 151 (2010).
22) Z.-C. Gu and X.-G. Wen, Phys. Rev. B **80**, 155131 (2009).
23) Z. Yang, L. Yang, J. Dai, and T. Xiang, Phys. Rev. Lett. **100**, 067203 (2008).
24) Z. H. Yang, L. P. Yang, H. N. Wu, J. Dai, and T. Xiang, Phys. Rev. B **79**, 214427 (2009).
25) L.-P. Yang, Y. Liu, H. Zou, Z. Y. Xie, and Y. Meurice, Phys. Rev. E **93**, 012138 (2016).
26) S. Wang, Z. Y. Xie, J. Chen, N. Bruce, and T. Xiang, Chin. Phys. Lett. **31**, 070503 (2014).